IEEE Access
Multidisciplinary | Rapid Review | Open Access Journal

Received 10 March 2024, accepted 4 April 2024, date of publication 8 April 2024, date of current version 15 April 2024.

Digital Object Identifier 10.1109/ACCESS.2024.3386092

RESEARCH ARTICLE

Harmonics Forecasting of Renewable Energy System Using Hybrid Model Based on LSTM and ANFIS

FAWAZ M. AL HADI AND HAMED H. ALY, (Senior Member, IEEE)
Department of Electrical and Computer Engineering, Dalhousie University, Halifax, NS B3H 4R2, Canada
Corresponding author: Hamed H. Aly (hamed.aly@dal.ca)

ABSTRACT Harmonics forecasting stands as a crucial approach in the development of devices aimed at minimizing harmonics disturbances. The primary objective of this study is to create a hybrid forecasting model that can deliver precise and dependable forecasts for harmonics in Renewable Energy Systems (RES). To achieve this goal, the Adaptive Neuro Fuzzy Inference System (ANFIS) with the Long Short-Term Memory Network (LSTM) are combined in two distinct structured models. In the first model, LSTM is employed in the initial stage and ANFIS in the subsequent one, while the second model follows the reverse order. Additionally, for the generation of harmonics, two renewable generator models are utilized. The first model encompasses a grid-connected Double-Fed Induction Generator (DFIG) driven by a wind turbine and integrated with a Solar Photovoltaic (PV)-based power generator. The second generator model combines a Solar-PV generator with a wind turbine-linked Permanent Magnet Synchronized Generator (PMSG) connected to a shared grid. The harmonics produced by these generator models are used to construct training and testing datasets, which are subsequently employed for generating forecasts using the proposed hybrid forecasting models. The accuracy of forecasting results is verified through a comparison with benchmark studies in the literature. The findings reveal that the model employing ANFIS in the initial stage and LSTM in the second stage (referred to as the ANFIS-LSTM model) consistently yields the best forecasts among all the models tested in this study with RMSE of 0.0287, 0.0372, 0.0396 and 0.0311 for THD, h7, h11 and h13 respectively. Moreover, it exhibits a significant improvement over any of the techniques used in previous literature. Ultimately, this research establishes that both hybrid models proposed outperform the individual forecasting techniques used as benchmarks in terms of accuracy and precision.

INDEX TERMS Harmonics, renewable energy systems, power quality, artificial neural networks, advanced neuro fuzzy inference system.

ABBREVIATIONS

DFIG	Double Fed Induction Generator.
PMSG	Permanent Magnet Synchronous Generator.
PV	Photovoltaic.
RES	Renewable Energy Systems.
EPS	Electrical Power System.
PQ	Power Quality.
PCC	Point of Common Coupling.
VSC	Voltage Source Converter.
THD	Total Harmonic Distortion.
TDD	Total Demand Distortion.
ANFIS	Adaptive Neuro Fuzzy Interference Systems.
LSTM	Long Short-Term Memory Network.
IEC	International Electrotechnical Commission.
IEEE	Institute for Electrical and Electronics Engineers.
FFT	The Fast Fourier Transform.
RMSE	Root Mean Square Error.
MAE	Mean Absolute Error.
MLPNN	Multilayer Perceptron Neural Network (MLPNN).

The associate editor coordinating the review of this manuscript and approving it for publication was Sotirios Goudos.

NARX	Nonlinear Autoregressive with Exogenous inputs.
LMS	Least Mean Square.
NLMS	Normalized LMS.
VLLMS	Variable Leaky Least Mean Square.
UDR	Univariate Dimension Reduction.
JRC	Joint Research Centre.

I. INTRODUCTION

The increasing demand for electrical power generated from renewable sources has becomes a critical concern. The widespread adoption of renewable energy technologies in the Electrical Power System (EPS) has led to the emergence of innovative concepts such as smart grids and microgrids [1]. One of the primary challenges in maintaining stability within the EPS, which directly impacts its Power Quality (PQ), arises from the unpredictable and uncontrollable nature of Renewable Energy Systems (RES) in terms of power generation. RES differ from traditional power sources due to their limited controllability, unfavorable power flow patterns, and non-sinusoidal current and voltage waveforms. Additionally, the integration of RES into the grid involves various power electronics-based converters and inverters [2], which introduce current and voltage harmonics into the grid [3]. These harmonics can have adverse effects, such as overheating transformers and causing issues in protection systems, among other factors [4]. Meeting the recommendations of IEEE 519-2014 [5] and adhering to IEC 61000 standards [6] is essential, with a particular emphasis on minimizing harmonics to ensure high network power quality. For instance, IEEE 519-2014 specifies that voltage Total Harmonic Distortion (THD) at the Point of Common Coupling (PCC) must not exceed a 5% limit [6].

Harmonics forecasting is one of the techniques used to design devices aimed at reducing harmonics [7]. Harmonics forecasting involves predicting the future behavior of time series data that exhibits periodic patterns or harmonics. A review of the literature indicates ongoing efforts to forecast harmonics, as it can significantly contribute to enhancing power quality. Various methods have been employed by researchers to achieve accurate predictions, including Adaptive Neuro Fuzzy Inference Systems (ANFIS) [8] and Long Short-Term Memory (LSTM) Network [9]. This research aims to develop and assess hybrid forecasting model capable of effectively capturing the intricate harmonic patterns in time series data and providing precise predictions. The study will focus on integrating a forecasting model that combines the strengths of ANFIS and LSTM to enhance the accuracy and reliability of harmonic forecasting. The integrated ANFIS-LSTM model is expected to proficiently handle the complex harmonic patterns in time series data and deliver accurate predictions.

Furthermore, the significance of this work extends beyond its immediate objectives and contributes to the broader context of harmonic mitigation within the realm of renewable energy systems. Harmonic mitigation is a critical aspect of power system engineering, aiming to minimize undesirable harmonic distortions in electrical waveforms. Standard techniques employed in harmonic mitigation include Passive Filters, Active Filters, Variable Frequency Drives (VFDs), Transformers with Low Harmonic Content or Power Factor Correction devices.

The novel contribution of harmonics forecasting, as presented in this work, lies in its potential application as a predictive tool to enhance the effectiveness of these standard harmonic mitigation techniques. By forecasting the occurrence and characteristics of harmonics, power system operators can implement preemptive measures to mitigate harmonics before they significantly impact the system. The role of harmonics forecasting in the harmonics mitigation process can be outlined as follows:

1. Proactive Planning: Harmonics forecasting provides insights into the expected harmonic content over time. This information allows for proactive planning, enabling the deployment of appropriate mitigation techniques in anticipation of periods with heightened harmonic levels.
2. Optimized Resource Allocation: Armed with harmonics forecasts, operators can allocate resources more efficiently. For instance, they can optimize the deployment of active filters or switch between different mitigation strategies based on the predicted harmonics profile.
3. Early Detection of Anomalies: Harmonics forecasting can serve as an early warning system by detecting deviations from expected harmonics patterns. This allows for timely investigation and intervention to address potential issues before they escalate.
4. Integration with Smart Grids: Harmonics forecasting aligns with the goals of smart grid integration. By incorporating forecasting capabilities into control systems, smart grids can dynamically adapt to changing harmonic conditions, enhancing overall system resilience.

In summary, the incorporation of harmonics forecasting into the broader context of harmonics mitigation enhances the adaptability and efficiency of conventional mitigation techniques. This proactive approach aligns with the evolving landscape of smart grid technologies and contributes to the advancement of strategies aimed at ensuring the stability and reliability of power systems in the presence of harmonics.

II. BACKGROUND

In the past, utility companies had a clear understanding of which industry their customers belonged to, especially those customers causing significant harmonic disturbances. Consequently, they used passive harmonic filters at the PCC for major distorting loads to address harmonic issues [10], [11], [12]. However, with the increasing integration of renewable energy sources into the grid, powered by various power electronics-based converters [13], [14], there has been a noticeable rise in power system harmonics. This has necessitated utilities to anticipate and mitigate the

effects of harmonics, requiring them to forecast the expected impact of these harmonics. To maintain power quality and ensure that harmonic levels remain within acceptable limits, researchers in the field have explored the concept of harmonic forecasting.

Ray et al. [15] introduced a harmonic forecasting method based on the Variable Leaky Least Mean Square (VLLMS). Kamenetsky and Widrow [16] algorithm. To prevent parameter drift, their method employed a compensating leak technique, and they also adjusted the step size to enhance convergence. Furthermore, they conducted real-time power system simulations using several examples to demonstrate the superiority of their approach compared to other methods mentioned in [15]. In [17], Ivry investigated how uncertainty affected harmonic prediction in a power system with numerous Voltage Source Converters (VSCs). They predicted the level of harmonic distortion at the PCC from the VSCs using the Univariate Dimension Reduction (UDR) approach. This approach ensured comprehensive modeling of interactions between the harmonic sources (VSCs) and the entire power system for predicting THD at the PCC. In [18], Hussam developed the concept of adaptive filters employing real-time harmonic prediction algorithms, employing approaches such as Least Mean Square (LMS), Normalized LMS (NLMS), and Recursive Least Square (RLS). These algorithms were used in an active filter to reduce the time delay associated with collecting harmonic information.

Pablo et al. [19] introduced an approach to estimate voltage THD for Low Voltage busbars of residential distribution feeders based on data from a limited number of smart meters. Various voltage THD forecasting methods, including feed-forward and autoregressive Artificial Neural Networks (ANN) et al. McCulloch and Pitts [20], were applied. This approach expanded the capabilities of existing monitoring tools for future harmonic distortion prediction. The study showed that a network of advanced smart meters, even with a small number of them, was sufficient for accurate harmonic estimations [18]. Furthermore, in [21], Mori and Suga proposed a technique for forecasting power system harmonic voltages using ANN, specifically Recurrent Neural Networks (RNN) et al. Hopfield [22]. They utilized four RNN models, including Jordan, Elman, Noda, and Nagao models, along with a fourth model featuring a context layer between the output and hidden layers as a separate recurrent network. The study found that Elman's technique outperformed the other models [21].

To monitor the effects of current harmonics generated by Photo-Voltaic (PV) systems, Žnidarec M. introduced predictive models for long-term current harmonic distortion in his research [23]. These models utilize a Multilayer Perceptron Neural Network (MLPNN) et al. Rosenblatt [24] to forecast current harmonics. Training data for the models included a year's worth of power quality measurements from the PCC of a 10-kW PV system and the distribution network, as well as meteorological data (solar irradiance and ambient temperature) collected at the test site. Six different models were developed, tested, and validated, varying in the number of hidden layers and input parameters. The fifth, seventh, eleventh, and thirteenth harmonics were predicted using these models, which utilized a three-phase grid-connected PV plant inverter along with MLPNN. The results indicated that including the third input parameter (time of day) marginally improved the MLPNN model's performance [23].

In a study by Panoiu and Ghiormez [25], they focused on modeling and predicting the THD of current in a medium voltage installation associated with an electric arc1 furnace. They employed ANFIS in MATLAB for modeling purposes. The findings revealed that ANFIS effectively learned how to adjust THD, achieving low error rates when extrapolating THD variation for an additional 400 examples after being trained on 800 data points. They also attempted to train the system with varying sample sizes but found that it did not perform well when the training data was smaller than the testing dataset [25].

Shengqing et al. [26] proposed a harmonic current prediction method using the Hybrid Active Power Filter (HAPF) based on Empirical Mode Decomposition (EMD) and Support Vector Regression (SVR). Cortes and Vapnik [27] theory to address microgrid power quality issues. This approach initially decomposed harmonic currents using EMD for each harmonic, then predicted the next-step harmonic currents at different time intervals using SVR with various kernel functions. Finally, they determined the weighted summation of the predicted values for each harmonic. Simulation results demonstrated the effectiveness of this EMD-SVR combination in accurately predicting harmonic currents at the next time step, leading to minimal harmonic current errors [26].

Kuyunani et al. [28] employed LSTM deep learning for voltage harmonics prediction. They utilized 8103 voltage harmonics samples from the Jeffreys Bay Wind Farm in the Eastern Cape Province to train their network. Their approach involved two steps: first, they collected essential data from voltage harmonics signals using moving window segmentation to determine the mean voltage amplitude. Then, based on the retrieved voltage attributes, they predicted voltage harmonic production using LSTM. The LSTM model achieved lowest error when predicting mean values for the following 3800 samples [28].

In their research, Hatata and Eladawy [29] employed a Nonlinear Autoregressive with Exogenous inputs (NARX). Chen and Billings [30] neural network to predict the occurrence of load current harmonics within electric power systems. They applied this technology in a microgrid located at the Khalda – Main Razzak power station in western Egypt, a facility associated with petroleum operations. The non-linear load under examination was an Electrical Submersible Pump, driven by an induction motor and controlled by a Variable Speed Drive. Their study outlined the process of developing the suggested NARX network, which aimed to replicate the behaviour of non-linear loads and compute

their THD in current. To evaluate the proposed network's performance, they tested it using both simulated pure sinusoidal voltage waveforms and actual measured voltage data, with the objective of determining the actual harmonic current of the load and assessing the nonlinearity of each load. Their findings indicated that the recommended NARX method outperformed the RNN-based approach, as they compared the two [29].

In their study, Pang [31] devised a method based on Stack Auto Encoder (SAE) Neural Networks for short-term harmonic forecasting and assessment influenced by electrified trains' impact on the power grid. Their aim was to predict harmonics and evaluate harmonic values using assessment techniques. The results of their study not only successfully achieved the goal of harmonic forecasting but also provided a theoretical framework for analysing the impact of railroads on harmonics. This framework holds the potential to enhance power quality within the power network.

In his study, Zavala and Messina [32] introduced a statistical framework for examining modal behaviour, extracting trends, and making forecasts using Dynamic Harmonic Regression (DHR). They evaluated the model's performance using both synthetic and observational data and applied it to wind power generation measurements to assess its practical applicability under various data gathering scenarios. The DHR model's forecasting function was demonstrated to be a valuable tool, capable of competing with other established techniques. It exhibited low forecasting errors that could be further reduced by selecting an appropriate moving window size.

Building upon the previous literature review, the primary aim of this research is to create an effective and dependable forecasting model for predicting harmonic fluctuations. To accomplish this objective, two hybrid forecasting models are proposed in this work, which are created by merging LSTM and ANFIS. The hybrid models are designed in two staged structures. First proposed model utilizes LSTM in the first stage and ANFIS in the second, whereas the second model is constructed the vice versa.

In the initial phase, two renewable generator models are employed to generate current and voltage harmonics. The first model utilizes a DFIG powered by a wind turbine combined with Photovoltaic panels (referred to as Wind DFIG-PV). The second model combines wind and photovoltaic sources using a PMSG. Subsequently, after obtaining the output waveforms, the harmonics are extracted from the data, which serve as the datasets for training and predicting harmonics using the proposed forecasting models.

III. RATIONALE TO BUILD HYBRID MODEL COMBINING ANFIS WITH LSTM FOR HARMONIC FORECASTING

The benefits and capabilities of each technique are the foundation for why a hybrid model for harmonic forecasting integrating LSTM and ANFIS should be constructed. It is possible to increase the forecasting model's accuracy and robustness by combining these two approaches and taking advantage of their respective benefits. Aspects for considering the hybrid strategy are presented as follows:

A. CAPTURING TEMPORAL DEPENDENCIES

LSTM is a powerful deep learning technique that excels in capturing long-term dependencies in time series data. It can effectively model the complex patterns and relationships within a sequence. By using LSTM, the hybrid model can leverage its ability to learn from historical harmonic data and capture the temporal dynamics of harmonic components.

B. FUZZY LOGIC-BASED REASONING

ANFIS is a fuzzy logic-based inference system that can handle uncertain and imprecise information. It combines the advantages of fuzzy logic and neural networks to create a hybrid model that can reason with linguistic rules and make inference based on fuzzy logic principles. This makes ANFIS suitable for handling complex, non-linear relationships and incorporating expert knowledge into the model.

C. INCORPORATING DOMAIN KNOWLEDGE

ANFIS allows the integration of expert knowledge in the form of linguistic rules. In the context of harmonic forecasting, domain experts may have insights and expertise that can contribute to accurate predictions. ANFIS can capture this expert knowledge and incorporate it into the forecasting process, complementing the data-driven approach of LSTM.

D. ENHANCED INTERPRETABILITY

ANFIS models are known for their interpretability. They provide linguistic rules that can be understood and analyzed by domain experts. This can be particularly useful in harmonic forecasting, where stakeholders may require explanations or justifications for the predictions. The hybrid model can provide interpretable results while benefiting from the powerful predictive capabilities of LSTM.

E. ROBUSTNESS AND GENERALIZATION

Combining different modelling techniques can enhance the robustness and generalization ability of the model. LSTM and ANFIS have different strengths and weaknesses, and by integrating them, the hybrid model can potentially overcome limitations and improve overall forecasting performance.

F. SUMMARY

A description of the model elements and their individual contributions to developing a hybrid model based on fusing LSTM and ANFIS for harmonic forecasting can be found in Table 1.

IV. GENERATOR MODELS

The simulation of hybrid models with a total capacity of 3 MW (1.5 MW wind generator plus 1.5 MW PV array) was performed in order to generate harmonics. To depict the real-world response, the actual wind speeds and solar irradiance

TABLE 1. Rationale for ANN-ANFIS based hybrid model summary.

Rationale	Long Short-term Memory Network	Adaptive Neuro-Fuzzy Inference System
Complementary strengths	Captures long-term dependencies and temporal patterns in sequential data.	Handles linguistic variables and interprets complex non-linear relationships in tabular data.
Improved accuracy	Enhances forecasting accuracy by leveraging LSTM's ability to capture temporal relationships.	Incorporates tabular features and fuzzy logic to capture additional contextual information.
Feature extraction and interpretation	Automatically learns feature representations from harmonic time series.	Utilizes tabular features directly and provides interpretability through fuzzy rules.
Robustness to data characteristics	Adapts to various data characteristics, such as seasonality and non-linear trends.	Model's complex non-linear relationships and adapts to linguistic variables in tabular data.
Ensemble effect	Harnesses ensemble benefits by combining LSTM with ANFIS for improved predictions.	Reduces the risk of overfitting and increases robustness and generalization performance.
Flexibility and customization	Enables customization by adjusting LSTM and ANFIS weights based on their performance.	Allows for customization according to specific harmonic forecasting requirements.

data were used as inputs for both hybrid models (Wind-DFIG-PV and Wind-PMSG-PV). Figures 1 & 2 show the generator models used in this work [33], [34].

The hybrid Wind-DFIG PV model combines the individual wind-DFIG model and PV model taken from MATLAB library. The Wind-DFIG Model contains 1.5 MW wind turbines using a wound rotor DFIG coupled with an AC/DC/AC IGBT-based PWM converter. The stator winding is connected directly to the 60 Hz grid while the rotor is fed at variable frequency through the AC/DC/AC converter. For low and high wind speeds the maximum extraction of energy is ensured by optimization of the turbine speed. In this model, the wind speed signal is being generated by a signal generator block. Furthermore, the PV model consists of a 1.5 MW rated PV array containing 518 parallel strings. Each string has 7 SunPower SPR-415E modules connected in series. The individual models for Wind-DFIG and PV were combined to be fed into the common grid. The grid is predefined in MATLAB model and is modelled as a typical distribution grid to add effect of a non-linear load. Thus, the grid acts as a non-linear load and may have some effect on the output harmonics of the model. Any variation caused by grid is not considered in this work. The focus is to simulate harmonics which are generated by the generator model and effects of variation in the renewable sources (Wind speed and Solar Irradiation) are studied.

Similarly, the hybrid Wind-PMSG PV model combines the individual Wind-PMSG model and PV model taken from MATLAB library. The Wind-PMSG model contains 1.5 MW wind turbines directly coupled with a multipole PMSG without a gearbox. The grid connection is established via an AC/DC/AC converter consisting of diode rectifier, internal DC-Link, and a Pulse Width Modulation (PWM) voltage-source inverter. This Wind-PMSG model was combined with a PV model and commonly fed into the grid as explained in the previous paragraph. The timestep for simulation is 5 microseconds and the overall time is scaled where one second in simulation represents 1 hour.

The wind speed, solar irradiance, and temperature readings were taken as actual data for Halifax, Nova Scotia, Canada, between June 1 and July 1, 2015, and logged into the signal generators. The data was obtained from the Joint Research Centre (JRC) of the European Commission [35]. The generator model was simulated for 31 days using the real-world data for wind speed and solar irradiation as inputs and producing output power. To store and use data for further analysis, the overall data portraying the variations in wind and solar parameters was split into datasets and the simulation was done in parts. Figure 3 and 4 presents a snapshot from the voltage waveform for Wind-DFIG PV generator with markers on phase 1, 2 and 3. The waveform which starts from 0 seconds is zoomed and snapped between 25 to 26 seconds to visualize the presence of harmonics in the voltage waveform:

Figure 3 shows the measurement markers on phase 1 and 2, while figure 4 shows marker positioned at phase 1 and 3. The voltage value is shown in the measurements window where it can be observed that the voltages of all 3 phases are balanced. The presence of harmonics can be observed from figures 3 & 4. Furthermore, to log data into the workspace, the MATLAB scope feature was used. Data was stored in format structure with time to further analyses. Moreover, a sample of the 3-phase current waveform is shown in Figures 5 and 6 zoomed and visualized between 15 and 16 seconds to demonstrate and visualize the presence of

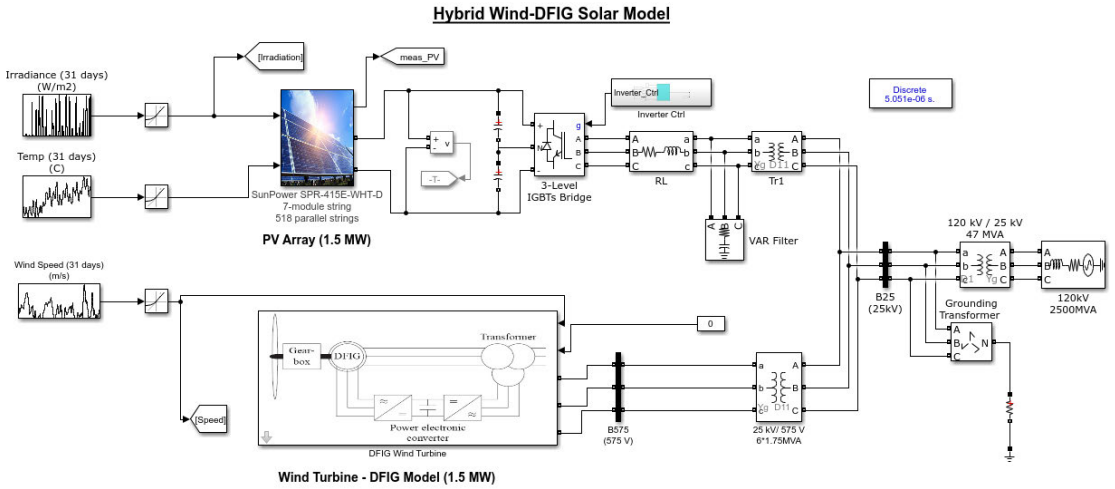

FIGURE 1. Wind-DFIG PV generator model.

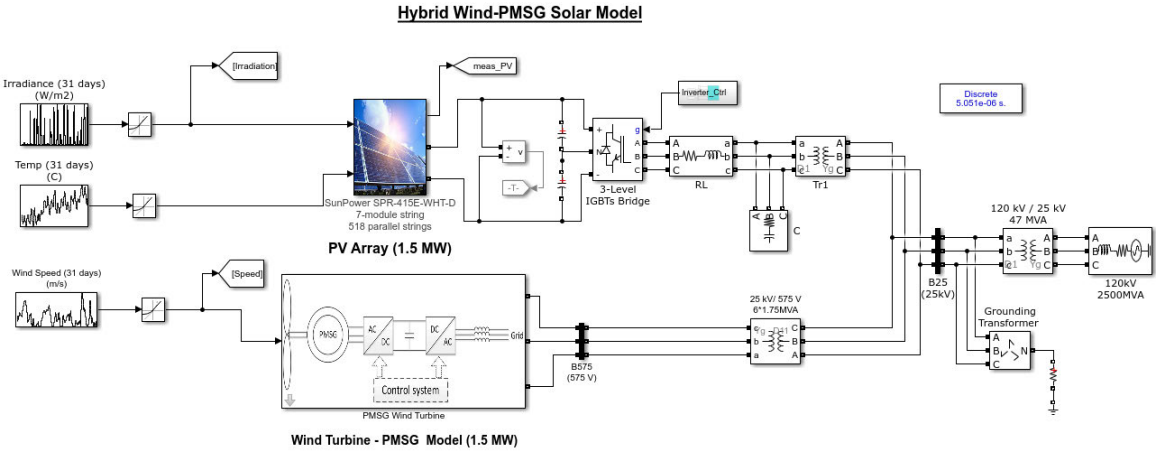

FIGURE 2. Wind-PMSG PV generator model.

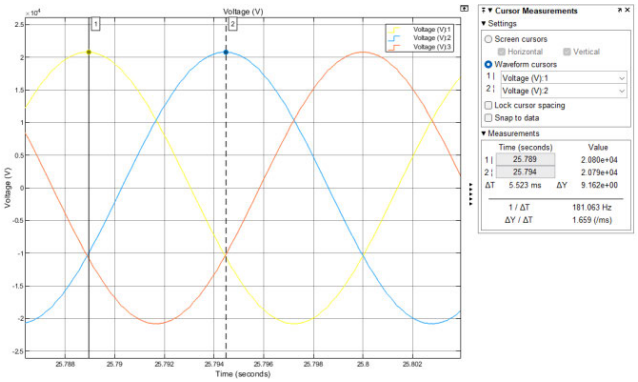

FIGURE 3. Sample voltage waveform for Wind-DFIG PV (Phase 1 & 2).

harmonics in the waveform generated for Wind-DFIG PV model. The presence of harmonics can be observed in current and voltage waveforms. Figure 5 shows markers on phase 1 & 2, whereas figure 6 points marker on phase 1 & 3. The value of current at marker can be seen in measurement window and appears to be equal. The focus will be kept on the phase one voltage and current waveforms to proceed further. All three-phase current waveforms are balanced, hence an in-depth analysis and forecasting on one phase is sufficient to realize the overall impact.

To extract harmonics, a Fast Fourier Transform (FFT) et al. Cooley and Tukey [36] analysis was carried out on the data procured from scope. The MATLAB command line was used to extract harmonic information. The FFT window employed consists of five cycles which extract the samples from voltage and current waveforms. The FFT samples were extracted for 720 hours (30 days), a total of 7200 samples were recorded with 10 samples logged per hour for both current and voltage waveforms. The following harmonic parameters were extracted from the simulated signals:

1. Total harmonic distortion for each sample
2. Magnitudes of 3rd, 5th, 7th, 9th, 11th & 13th harmonic component

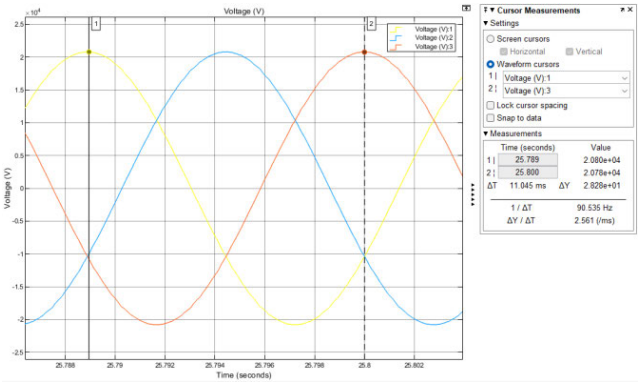

FIGURE 4. Sample voltage waveform for Wind-DFIG PV (Phase 1 & 3).

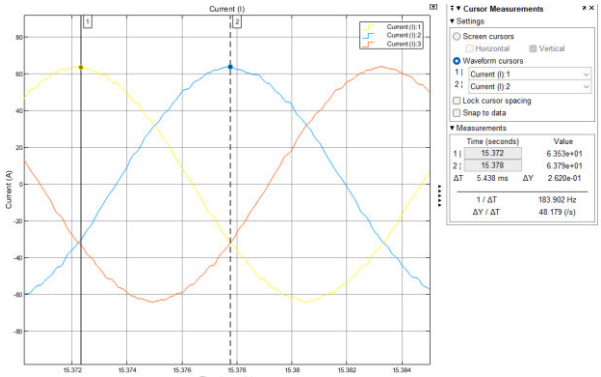

FIGURE 5. Sample current waveform for Wind-DFIG PV (Phase 1 & 2).

V. FORECASTING MODELS

A. ADAPTIVE NEURO FUZZY INFERENCE SYSTEM (ANFIS)

In the early 1990s, the ANFIS was created because of Jang Roger's [8] proposal to combine ANN and Fuzzy Logic. Based on the Takagi-Sugeno Fuzzy Inference System et al. Takagi and Sugeno [37], ANFIS combines the durability, ease of use, and convenience of implementing the rule bases of the fuzzy system with the self-learning characteristics of ANN. The ANFIS systems are particularly efficient and straightforward to build, especially in circumstances where non-linearity and data uncertainty are problems [38]. Eq. (1) demonstrates a typical fuzzy rule in a Sugeno fuzzy model:

$$IF\ x\ is\ A\ and\ y\ is\ B,\ THEN\ z = f\ (x, y) \tag{1}$$

where A and B are fuzzy sets, z = f (x, y) is a crisp function defining the output. The function f (x, y) is typically a polynomial which describes the output based on the input variables x and y within the fuzzy region specified by the fuzzy sets of the rule [38]. Considering a first order Sugeno Fuzzy Inference System (FIS) which contains two rules expressed in (2) [38]:

$$\begin{aligned} &Rule1: IF\ x\ is\ A1\ and\ y\ is\ B1,\ THEN\ f1 = p1x + q1y + r1 \\ &Rule2: IF\ x\ is\ A2\ and\ y\ is\ B2, THEN\ f2 = p2x + q2y + r2 \end{aligned} \tag{2}$$

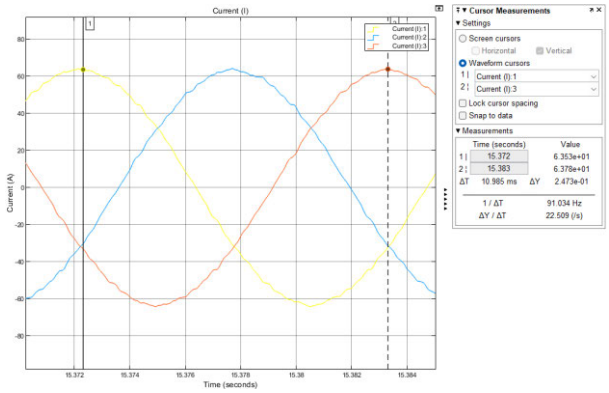

FIGURE 6. Sample current waveform for Wind-DFIG PV (Phase 1 & 3).

The final output is a summation of all incoming signals expressed as follows:

$$f = \sum_i \bar{w}_i f_i = \frac{\sum_i \bar{w}_i f_i}{\sum_i \bar{w}_i} \tag{3}$$

where, f_i is the output within the fuzzy region specified by the fuzzy rule and w_i is the assigned weight.

B. LONG SHORT-TERM MEMORY NETWORK (LSTM)

LSTM is a RNN architecture that was proposed by Hochreiter and Hochreiter and Schmidhuber in [9]. The core idea behind LSTM is to have a memory cell that can store information for a long time and selectively decide what information to keep and what to discard. LSTMs have been successfully applied to various tasks such as speech recognition, image captioning, natural language processing, and time series forecasting.

Recurrent neural networks, which form the basis of LSTM networks, are effective because they can recognize long-term relationships. Small weights are frequently multiplied repeatedly through a few steps in an RNN, and as a result, the gradients asymptotically approach zero. The vanishing gradient problem is another name for this RNN flaw. Cells, the memory units that make up the LSTM network, are connected by layers. In these cells, the data is present in both the cell state C_t and the hidden state ht. This information is governed by gates through the sigmoid, and tanh acts as the activation function. Integers between 0 and 1 are commonly produced using the sigmoid function, with 0 denoting no information flowing through and 1 denoting that this is the focus. Long short-term memory networks can conditionally add or remove information from the cell state as a result. In essence, the gates take the input, the hidden states from the previous time step (h_{t-1}), and the current input (x_t), multiplying them pointwise by weight matrices (ω), and then adding bias (b) to the result. The three primary gates are the forgetting gate, input gate and output gate. The forget gate, which decides the data to be removed from a specific cell state, outputs a number between 0 and 1, with 0 denoting complete deletion and 1 denoting complete retention [9]. The

following is provided in equation (4):

$$f_t = \sigma\left(\omega_f\left[h_{t-1}, x_t\right] + b_f\right) \tag{4}$$

The input gate which has a *tanh* activation layer that produces a vector of prospective candidates as shown in the following equation:

$$\hat{C}_t = \tanh\left(\omega_c\left[h_{t-1}, x_t\right] + b_c\right) \tag{5}$$

The sigmoid layer can then construct the following update filter as a result:

$$U_t = \sigma\left(\omega_u\left[h_{t-1}, x_t\right] + b_u\right) \tag{6}$$

The previous cell state, C_{t-1}, was then updated to:

$$C_t = f_t * C_{t-1} + U_t \times C_t^* \tag{7}$$

The output gate, which filters the cell state going to the output, is the last step. It has a sigmoid layer. The equation provides the following:

$$O_t = \sigma\left(\omega_0\left[h_{t-1}, x_t\right] + b_0\right) \tag{8}$$

The numbers are then scaled to fall between $[-1, 1]$ by using the tanh function on the cell state C_t. According to the equation, the new hidden state is made by multiplying the scaled cell state by the filtered output and then being transferred to the next cell.

$$h_t = O_t \times \tanh\left(C_t\right) \tag{9}$$

C. NOVEL HYBRID FORECASTING MODELS

There are two hybrid forecasting models proposed in this work by combining ANFIS and LSTM techniques. The concept design of these models is depicted in Fig. 7 & 8.

VI. METHODOLOGY FOR IMPLEMENTATION OF FORECASTING MODELS

A. DATA GENERATION FROM GENERATOR MODELS

To generate harmonic forecasts using the proposed hybrid models, the two generator models were simulated for 31 days. Real-time data for wind speed and solar irradiation for Halifax was used as recorded between June 1st and July 1st, 2015 [35]. The generator models produce output voltage and current waveforms from which harmonics were extracted using FFT. This harmonic data was further analyzed and stored to be used as inputs for the forecasting models. The data for the 30 days (June 1st to 30th, 2015) was used for training and formed the training set, while the data for 1 day (July 1st, 2015) was used as test set.

B. SELECTION OF INPUTS

The selection of input is crucial to achieve accurate forecast. Inputs shall be carefully selected from the available data by analyzing the trends for the target signal. To extract harmonics, an FFT analysis was carried out on the data procured from scope. The MATLAB command line was used to extract harmonic information. The FFT window employed

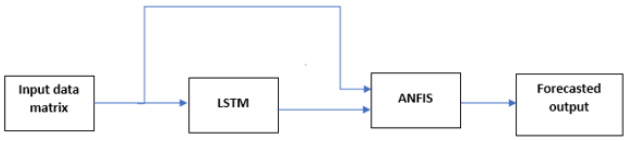

FIGURE 7. LSTM-ANFIS model (Model-1).

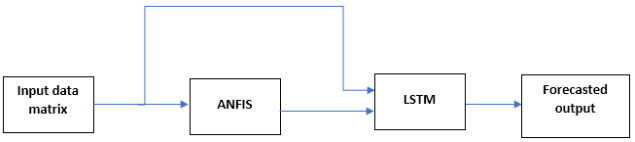

FIGURE 8. ANFIS-LSTM model (Model-2).

consists of 5 cycles which extracts the samples from voltage and current waveforms. The FFT samples were extracted for 720 hours (30 days), a total of 7200 samples were recorded with 10 samples logged per hour for both current and voltage waveforms. The following harmonic parameters were extracted from the simulated signals which after statistical analysis were selected as parameters to be forecasted for both voltage and current waveforms:

1. Total Harmonic Distortion (THD) / Total Demand Distortion (TDD)
2. Magnitude of 7th (h7) harmonic component.
3. Magnitude of 11th (h11) harmonic component.
4. Magnitude of 13th (h13) harmonic component.

Additionally, the forecasting models employ various amounts of parameters for input variables (predictors) which are used as inputs to produce forecast. They are stated as follows:

1. Wind Speed
2. Solar Irradiation
3. One Hour before observation of predicted parameter
4. One day before observation of predicted parameter
5. Two days before observation of predicted parameter

The selection of wind and solar irradiation was obvious as the forecasted parameters (THD/TDD, 7th, 11th, or 13th harmonic) directly depend on magnitude if wind or solar irradiation. As for the historical parameters, the one hour, one day and two days before observations, the predicted parameter has no dependencies on these inputs but rather related as at these time intervals the conditions were observed to be similar. In order to illustrate the correlation, Figure 9 presents the plot for voltage harmonics forecasting parameter, THD for Wind-DFIG PV generator model.

In figure the THD for day 5 is plotted against the THD value for one hour before, one day before and two days before. The patterns appear to be similar trajectory hence they are selected as input for forecasting model. With the training methodology adopted, the weight adjustment shall be able to train the network to produce accurate forecasts. In further analysis to inputs, day 5 and 4 wind speed and solar irradiation are plotted against respective THD in figures 10 and 11.

It can be observed that the change in both wind speed and solar irradiation have proportionate effect on total harmonic distortion. For instance, in figure 10 at 9 seconds the solar irradiation and wind speed both start to increase which also result in increasing the THD.

The increment in THD with small increase in magnitude of THD in figure 10. In figure 11, which shows the day 4 curves, at time of 1 seconds the wind speed increases and then falls resulting in a similar increment and dip in THD curve. Similar changes can be observed in the trajectory of THD with respective changes in wind speed and solar irradiation. Hence these parameters are also selected as an input in forecasting model to train it and adjust weights accordingly to produce forecast.

C. DATA PRE-PROCESSING

Data pre-processing is a step in which all data points are normalized between values of 0 and 1. This simplifies the calculations and uniformly presents all input parameters under one scale [9]. For ANN and ANFIS implementation, it is necessary to normalize data this way for better convergence. The following formula is used to normalize data:

$$x_{norm} = \frac{x - x_{min}}{x_{max} - x_{min}} \tag{10}$$

where,

x_{norm} is the normalized data point
x is the actual data point
x_{min} the minimum data point in the series
x_{max} the maximum data point in the series

Furthermore, data standardization is the process of transforming data into a common scale or format that involves rescaling the data to have zero mean and unit variance. In the context of LSTM models, data standardization is crucial to ensure optimal performance and convergence during training and prediction. Data standardization is done by subtracting the mean value of the data and dividing by the standard deviation, as explained in the following steps.

1. Compute the mean (μ) of the data: Calculate the average of all data points in the dataset.
2. Compute the standard deviation (σ) of the data: Calculate the square root of the average of the squared differences between each data point and the mean.
3. Subtract the mean from each data point: For each data point (x), subtract the mean (μ) from it.
4. Divide the mean-adjusted values by the standard deviation: Divide each mean-adjusted data point by the standard deviation (σ).

This can be represented by the formula:

$$x_{standardized} = \frac{x - \mu}{\sigma} \tag{11}$$

where,

$x_{standardized}$ = standardized dataset,
x = data set,
μ = mean value of the dataset, and

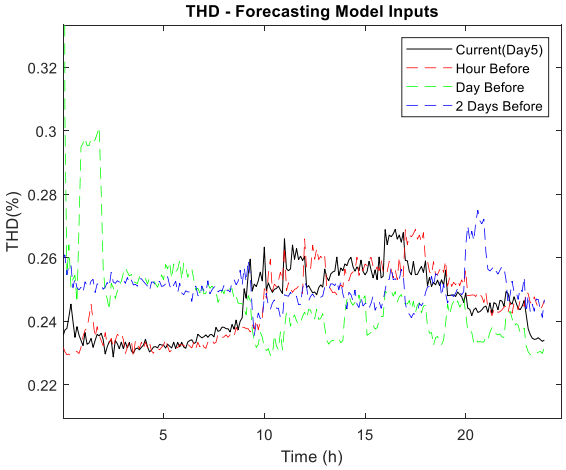

FIGURE 9. Total harmonic distortion curves for wind-DFIG PV model.

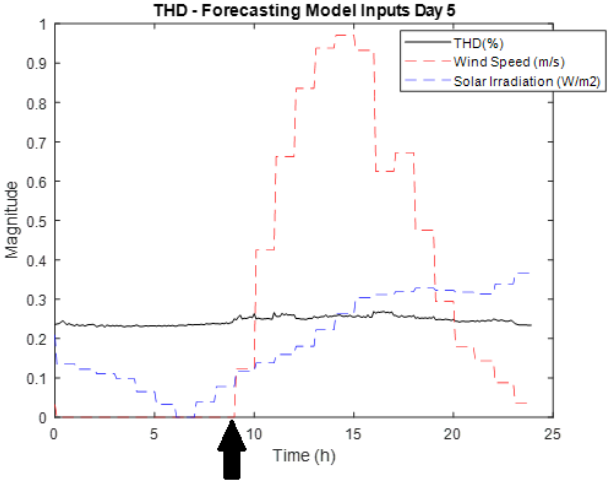

FIGURE 10. Total harmonic distortion vs wind speed and solar irradiation curves day 5 for wind-DFIG PV model.

σ = standard deviation of the dataset.

Data standardization for LSTM is crucial for facilitating convergence, avoiding gradient-related issues, treating features equally, and improving the generalization and performance of the model. By standardizing the data, you ensure that the LSTM model can effectively learn and make accurate predictions on a wide range of inputs [9].

D. NETWORK TRAINING AND FORECASTING

1) APPLICATION OF ADAPTIVE NEURO FUZZY INFERENCE SYSTEM (ANFIS)

ANFIS is a hybrid system that combines the advantages of both ANN and the fuzzy system [39]. As a result, ANFIS is more accurate at making predictions than ANN. To model data uncertainty, ANFIS essentially combines the learning capabilities of NNs with those of FIS, making it relatively easy to train an ANFIS model without the need for detailed subject-matter expertise. Furthermore, ANFIS has the benefit of utilizing both verbal and numerical information. Thus, the

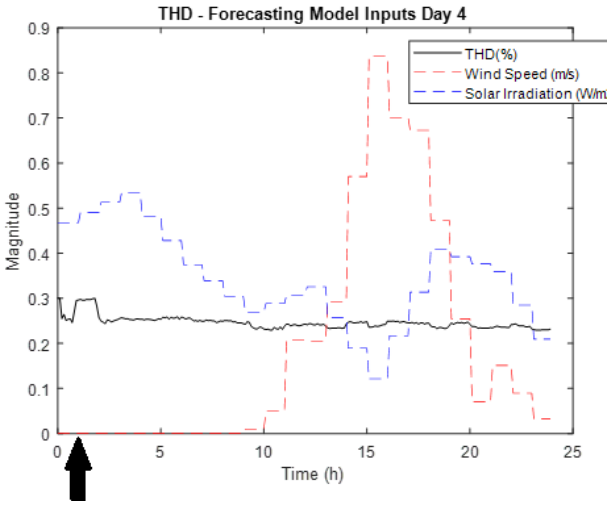

FIGURE 11. Total harmonic distortion vs wind speed and solar irradiation curves day 5 for wind-DFIG PV model.

flexibility, nonlinearity, and quick learning of ANFIS are its benefits.

However, the system becomes exceedingly challenging to execute when the number of inputs to the standard ANFIS's fuzzy system rises. Additionally, the more inputs and membership functions are selected, the more training time is needed, and increases in the number of membership functions per input subsequently increases the fuzzy rules. However, applying the ANFIS method for prediction, which is based on clustering, makes it simple to overcome these challenges.

Subtractive clustering is a prediction-making procedure that determines the number of clusters and their centre. It is also useful when data characteristics make clustering uncertain. The subtractive clustering method is an extension of the mountain clustering method proposed in [40]. In subtractive clustering, each data point is first evaluated as a prospective cluster centre candidate, after which each data point's potential is determined by calculating the density of the data points around it. This strategy is helpful in cases where it is unclear how many data distribution centres will be needed.

This work uses subtractive clustering. Because the approach is iterative, it assumes that any point could serve as the centre of a cluster, depending on where it is in relation to other data points. Subtractive clustering involves selecting the point with the best likelihood of being the cluster centre, then deleting every other point inside the first cluster centre's radius (the radius being defined by the neighbourhoods of the centre). To find the next cluster's centre, the potential of the other spots is recalculated. The calculation proceeds until all the data are contained within a cluster centre's radius [41]. A step-by-step overview of the process is given below.

1. Based on the density of nearby data points, determine the likelihood that each data point would define a cluster centre. Measure density index D_i corresponding to data x_i as expressed in (12) [41].

$$D_i = \sum_{j=1}^{n} \exp\left(-\frac{\|x_i - x_j\|^2}{\left(r_a/2\right)^2}\right) \tag{12}$$

where,

r_a = positive number that represents the radius where all the data within it are considered neighbourhoods.

2. Pick the data point that has the best chance of becoming the first cluster centre. Hence, the data point with the highest density measure is selected as the first centre cluster denoted x_{c1} and its density is D_{c1}.
3. Eliminate all data points close to the first cluster centre. With the use of cluster influence range, the area is identified.
4. Recalculate the density measurements for each data point xi and select the final point with the greatest potential to serve as the cluster centre expressed in (13) [41].

$$D_i' = D_i - D_{cl} \exp\left(-\frac{\|x_i - x_{c1}\|^2}{\left(r_b/2\right)^2}\right) \tag{13}$$

where,

$r_b = \mathrm{K} r_a$ (K is a positive number, usually K = 1.5 [41]).

All the points near to the first cluster centre x_{c1} will have low-density degree and thus they will not be considered as the next cluster centres. The next cluster centre x_{c2} is nominated after the density measure for each data point is recalculated.

5. Keep going back and forth between steps 3 and 4 until a cluster centre can affect all the data.

For optimization, the following parameters were changes to improve the performance. Specify the following clustering options:

- Squash factor - Only find clusters that are far from each other.
- Accept ratio - Only accept data points with a strong potential for being cluster centres.
- Reject ratio - Reject data points if they do not have a strong potential for being cluster centres.

In this work, the ANFIS is utilized using subtractive clustering which is optimized by trial and error.

2) APPLICATION OF LONG SHORT-TERM MEMORY NETWORK (LSTM)

The LSTM model employed within this study comprises five sequential input layers, each dedicated to an individual input. It also includes 100 LSTM layers, organized as 20 hidden layers per input, and further incorporates a fully connected layer and a regression layer serving as the output layer. The input layer's dimensions align with the number of inputs, which is set at five. This configuration facilitates the deployment of a cumulative total of 100 LSTM layers, employed to facilitate additive interactions and the acquisition of intricate enduring relationships within sequence and time series data. To adapt to varying input dimensions, the fully connected layer employs an 'auto' setting to automatically discern the

number of inputs received from the LSTM layer, executing matrix multiplication and bias vector addition as part of its operations. The regression layer is responsible for training and computational tasks, ultimately yielding the network's output. Figure 12 presents a visual representation of the LSTM network and the architecture utilized in this study.

E. K-FOLD CROSS VALIDATION

Cross-validation is a widely used technique for model evaluation, and its adaptation to time series data is crucial due to the sequential nature of such data. K-fold cross-validation et al. Ron [42] is a resampling method used to assess how well a model performs on a certain dataset. The dataset is divided into K folds of equal size. The model is tested on the remaining fold after being verified on K-1 folds. Each fold serves as the validation set precisely once during the K-fold iteration of this process. The model's overall performance is then evaluated by averaging the performance metrics received from each fold.

Furthermore, time series forecasting seeks to make future value predictions using data from the past. Each observation in a time series data set is influenced by earlier observations due to its temporal dependencies. Applying cross-validation techniques presents specific issues because of this sequential nature. As a result, the typical cross-validation approach is inapplicable to time series data since it implies that data points are independent and equally distributed. Due to the intrinsic temporal interdependence of time series, random data splitting or rearranging can cause information leakage and produce unduly optimistic performance predictions. A modified form of K-fold cross-validation is utilized to overcome the difficulties presented by time series data. The main concept is to keep the data's temporal order during cross-validation. Utilizing an expanding window system, which mimics the real-time forecasting scenario, is one popular strategy. For time series data, the expanding window method is a K-fold cross-validation variant. The training data window is gradually expanded throughout each fold to make sure the model is trained on historical data before generating predictions for upcoming time steps [42].

The K-Fold cross validation is applied on all the proposed models to improve training. The expanding window variation of K-fold is used. In this work data for 30 days is used to train the networks using K-fold cross validation with the value of K selected as 5. The application of K-fold is explained in following steps:

1. The initial training window size is set to 25.
2. Split the time series data into K (5) folds as shown in figure 28. The value of K is selected based on the tests performed by setting K between 5 and 10. With K equal to 5, the training error achieved remains almost the same with higher values of K. Also, with high K, the computation time is much longer with no significant advantage. Hence K-5 was found to result in low training error with lesser simulation time.

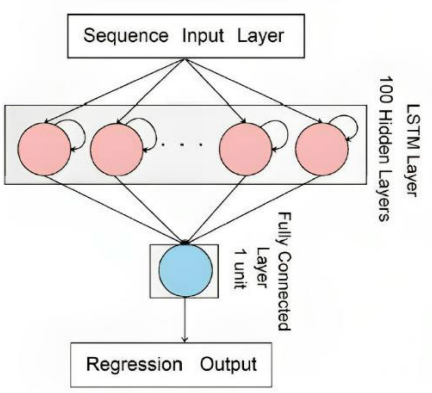

FIGURE 12. Structure of LSTM model.

3. For each fold:
   a. The model is trained using the data from the start of the time series up to the end of the current fold.
   b. Predict the next time step (day) using the trained model.
   c. Evaluate the performance of the model for the current fold.
   d. Slide the training window forward by one time step (day), incorporating the current fold's data.
4. Repeat steps 3a to 3d for all K (5) folds.
5. Aggregate the performance metrics obtained from each fold to assess the overall model performance. Using this approach, all past data is assigned to the training set and successively consider each day as the test set. Using the 30-day length of the dataset and 5 folds, five distinct training and test divides are created, as illustrated in the figure 13. With this method, a variety of train/test splits are generated, and the error on each split is averaged to obtain a reliable estimate of the model error. In this way the weights are adjusted to produce the most accurate forecast and the model is trained and ready to be evaluated. The approach is presented in figure 14.
6. The final step is to forecast for day 31. The trained model with weights adjusted and improved via K-fold technique is evaluated with test data to produce forecast. Figure 14 summarizes the whole process from steps 1 to 6 which is adopted in this work to produce forecasting results using the proposed hybrid models.

F. HYBRID FORECASTING MODELS: LSTM-ANFIS MODEL & ANFIS-LSTM MODEL

The proposed LSTM-ANFIS uses LSTM for forecasting in stage one and ANFIS in stage two. The five inputs are sent to the sequence input layer of LSTM. The LSTM model contains five input layers, a hundred hidden layers in the LSTM layer, one fully connected layer and a regression layer as output layer. K-fold validation is during training and the final forecast produced serves as input for stage two of the LSTM-ANFIS model. In stage two ANFIS received input from LSTM model plus the five inputs used to predict day 31 harmonics. K-fold technique us utilized for ANFIS training

along with subtractive clustering of the data. In this way ANFIS stage produces the final forecast for LSTM-ANFIS.

Furthermore, ANFIS-LSTM model utilizes ANFIS model in stage one and LSTM model in stage two. ANFIS produces forecasting results which are sent to LSTM model. The LSTM network receives six inputs including the five input parameters and sixth from output of ANFIS model. In this way the LSTM network consist of six input layers, 120 hidden layers in LSTM layer, one fully connected layer and a regression layer to produce the final output which is the forecast for 31st day.

G. EVALUATION OF FORECASTING MODELS

The performance of forecasting models is evaluated using the Mean Absolute Error (MAE) et al. Willmott and Matsuura [43] and Root Mean Squared Error (RMSE) et al. Chai and Draxler [44] indices. When a model's MAE and RMSE are both smaller, it performs better. With time step N, target sequence denoted by t_i while forecast sequence by f_i, i denotes the datapoint, (14) and (15) presents the formulas to calculate the RMSE and MAE:

$$RMSE = \sqrt{\frac{1}{N}\sum_{i=1}^{N}(t_i - f_i)^2} \tag{14}$$

$$MAE = \frac{1}{N}\sum_{i=1}^{N}|t_i - f_i| \tag{15}$$

Furthermore, MAPE et al. Myttenaere and Golden [45] is also often used as measurement metric for forecasting. It is a percentage-based metric that calculates the average percentage difference between predicted and actual values. It is particularly useful for expressing forecasting accuracy in terms of percentage errors, making it interpretable and comparable across different datasets. However, in this work RMSE and MAE are used as forecasting performance indicators. The choice of evaluation metrics in forecasting studies is often influenced by the specific characteristics of the problem and the goals of the research. In the context of harmonic forecasting, the decision not to use MAPE (Mean Absolute Percentage Error) may be attributed to several considerations.

1. Sensitivity to Outliers: MAPE and SMAPE can be sensitive to outliers, especially in the presence of extreme values. Harmonic forecasting, which deals with periodic patterns, may involve data points that deviate significantly from the average. An evaluation metric less sensitive to outliers might be preferred to provide a more robust assessment of forecasting accuracy.
2. Seasonal Patterns: The nature of harmonic forecasting involves capturing seasonal or periodic variations. Traditional metrics like MAPE and SMAPE may not fully account for the unique characteristics of harmonic patterns, leading to potential inaccuracies in assessing the model's performance.
3. Assumption of Symmetry: SMAPE assumes symmetry in percentage errors, which may not hold true in all forecasting scenarios. In harmonic forecasting, where irregularities and asymmetries in the data may be common, a metric that does not make strict symmetry assumptions might be more appropriate.
4. Research Objectives: The researchers may have specific objectives or hypotheses guiding their study that necessitate the use of alternative metrics. For instance, they may be focusing on minimizing errors during peak periods or emphasizing accurate forecasting for specific harmonic components, which could warrant the use of specialized metrics.
5. Comparison with Previous Studies: The decision to use or not use certain metrics could be influenced by the desire to compare results with previous studies in the field. If other harmonic forecasting studies have demonstrated the limitations of MAPE or SMAPE in this context, the researchers might opt for more suitable metrics to ensure consistency in the literature.

In the absence of specific information from the paper, these points provide a general perspective on why MAE and RMSE are preferred over MAPE for harmonic forecasting.

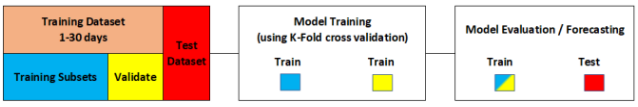

FIGURE 13. K-Fold cross validation process for model training.

FIGURE 14. Forecasting using K-Fold cross validation for model training.

VII. RESULTS AND ANALYSIS

In this section, the forecasting results are presented. To validate forecasting results, they are compared with forecasting techniques adopted in the literature by other authors. Three Neural Networks are chosen from among the methods used in [19], [21], and [23] to accomplish the forecasting for this work. Cascaded Recurrent Neural Network with Local Feedback (CRNNL), Cascaded Recurrent Neural Network with Global Feedback (CRNNG), and Cascaded Recurrent Neural Network with Local and Global Feedback (CRNNGL) are these networks. In addition, references [28] used the LSTM approach for prediction, whereas reference [25] uses ANFIS for forecasting. These 5 approaches are used to draw a comparative analysis in which the same data used in this work is utilized for all different forecasting methods stated. RMSE and MAE are the indices used to compare the results.

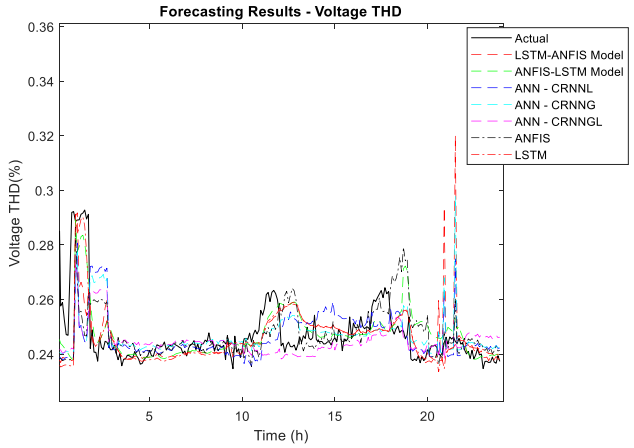

FIGURE 15. THD – actual vs forecast curves Wind DFIG-PV.

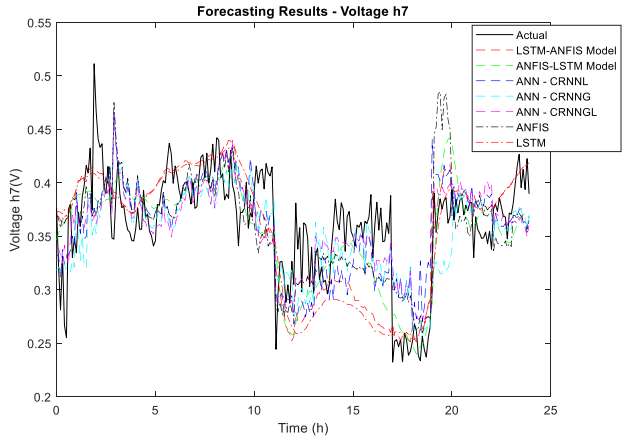

FIGURE 16. Voltage 7^{th} harmonic – actual vs forecast curves wind DFIG_PV.

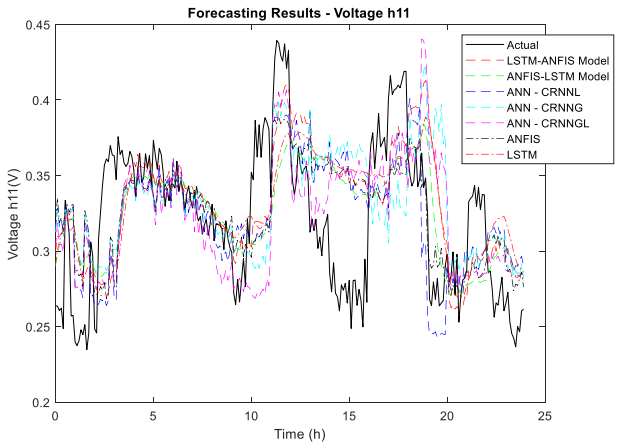

FIGURE 17. Voltage 11^{th} harmonic – actual vs forecast curves wind DFIG_PV.

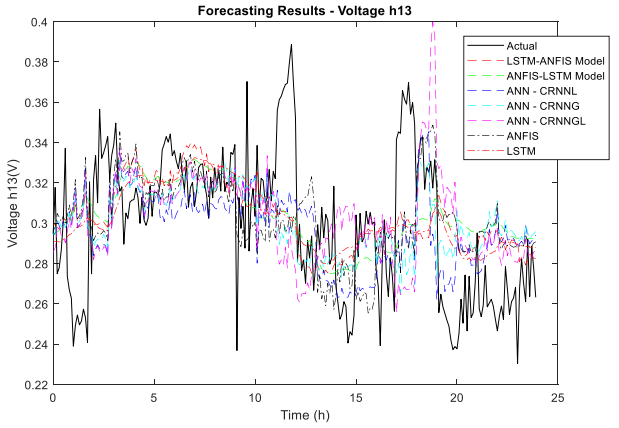

FIGURE 18. Voltage 13^{th} harmonic – actual vs forecast curves wind DFIG_PV.

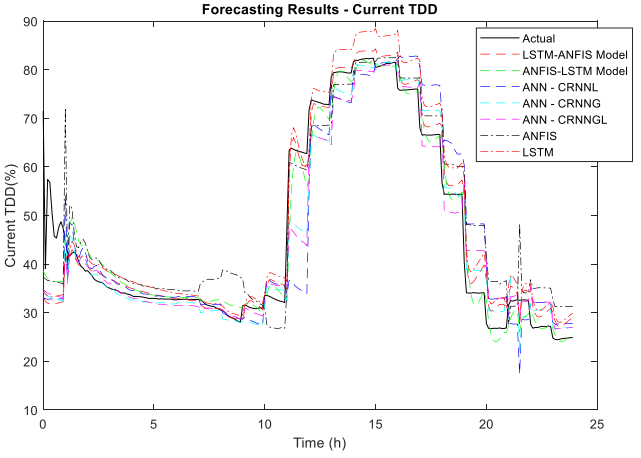

FIGURE 19. TDD – actual vs forecast curves wind DFIG-PV.

A. HARMONIC FORECASTING – WIND DFIG-PV MODEL

1) VOLTAGE HARMONICS

The actual versus forecast curves for all eight proposed hybrid models for wind DFIG-PV are presented in figures 15, 16, 17 & 18 along with the forecasting result curves of all the forecasting techniques found in literature i.e., ANN – CRNNL, ANN – CRNNG, ANN – CRNNGL LSTM and ANFIS. There are a total of four harmonic variables that have been forecasted, the THD followed by the dominant individual harmonics 7^{th} (h7), 11^{th} (h11) and 13^{th} (h13).

To further analyze the error profile and accuracy of these models and validate results, Table 13 presents the metrics calculated (RMSE & MAE) for eight proposed models in this research and forecasting techniques employed by other researchers in the literature. From Table 2 it can be observed that ANFIS-LSTM model produces the best results with the lowest RMSE & MAE for THD (0.0287 & 0.0076), h7 (0.0372 & 0.03), h11 (0.0396 & 0.0324) and h13 (0.0311 & 0.0250) forecast, while LSTM-ANFIS model produces the second-best results for all predictors respectively. It is obvious that ANFIS-LSTM model is the most accurate forecasting model for all the voltage harmonic forecasting parameters as it produces the best performance.

Furthermore, the results produced by forecasting techniques used in literature are also stated in table 2. By contrasting the results with CRNNL, CRNNG, CRNNGL, LSTM and

TABLE 2. THD, 7th, 11th and 13th voltage harmonics forecast results for wind DFIG-PV model.

Forecasting Models	THD		h7		h11		h13		Reference / Publication
	RMSE	MAE	RMSE	MAE	RMSE	MAE	RMSE	MAE	
LSTM-ANFIS Model	0.0295	0.0077	0.0403	0.0328	0.0428	0.0346	0.0318	0.0256	Proposed Model
ANFIS-LSTM Model	**0.0287**	**0.0076**	**0.0372**	**0.0300**	**0.0396**	**0.0324**	**0.0311**	**0.0250**	Proposed Model
LSTM	0.0305	0.0095	0.0459	0.0344	0.0470	0.0380	0.0368	0.0273	[27]
ANFIS	0.0306	0.0099	0.0423	0.0342	0.0448	0.0371	0.0378	0.0297	[26]
CRNNL	0.0310	0.0104	0.0427	0.0329	0.0489	0.0357	0.0396	0.0314	[22], [23] & [24]
CRNNG	0.0307	0.0101	0.0481	0.0368	0.0526	0.0417	0.0394	0.0296	[22], [23] & [24]
CRNNGL	0.0321	0.0121	0.0442	0.0360	0.0473	0.0370	0.0388	0.0294	[22], [23] & [24]

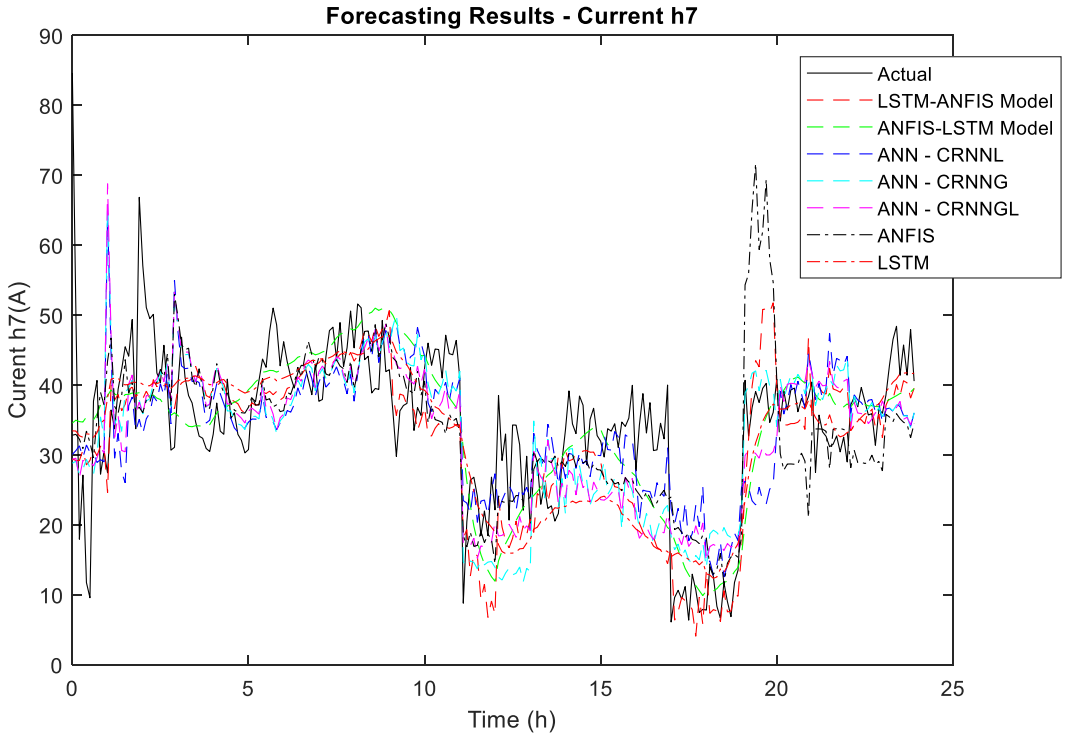

FIGURE 20. Current 7th harmonic – actual vs forecast curves wind DFIG_PV.

ANFIS, the benefit of utilizing hybrid technique can be realized. For THD and h13, LSTM produces the most accurate forecasting result (RMSE – 0.0301 for THD & 0.0368 for h13) as compared to all other forecasting techniques. Moreover, for h7 and h11, ANFIS appears to be the most accurate individual forecasting model with RMSE 0.0423 for h7 and 0.0448 for h11 respectively. Even though LSTM and ANFIS perform best among all individual models tested, the results produced by hybrid models surpass the accuracy. Additionally, the ANFIS-LSTM model manifests the best forecasting results. Furthermore, LSTM (THD & h13) and ANFIS (h7 and h11) have been better performing models among the individual forecasting techniques. A percent improvement that ANFIS-LSTM model offers as compared to all the singular models in literature tested in this work is presented in table 3 to validate the results and illustrate the benefit of utilizing hybrid model over singular models.

It can be observed that ANFIS-LSTM Model offers improvements over all the individual models. For instance, for THD and h13 the model offers 4.46% and 15.51% improvement over LSTM forecast respectively. Similarly, for h7 and h11, 12.03% and 11.53% improvement are recorded over ANFIS which is the best performing model for h7 and h11. Likewise, the percent improvement demonstrated by ANFIS-LSTM model over all other models is evident and establishes the superiority of proposed hybrid models over forecasting techniques used in literature.

TABLE 3. Best forecasting model comparison for voltage harmonics – wind DFIG-PV.

Forecasting Parameter	ANFIS-LSTM Model RMSE	RMSE (% Improvement)				
		LSTM	ANFIS	CRNNL	CRNNG	CRNNGL
THD	0.0287	0.0301 **(4.46%)**	0.0305 **(5.9%)**	0.0301 **(7.48%)**	0.0307 **(6.56%)**	0.0321 **(10.63%)**
h7	0.0372	0.0459 **(18.97%)**	0.0423 **(12.03%)**	0.0427 **(12.98%)**	0.0481 **(22.67%)**	0.0442 **(15.96%)**
h11	0.0396	0.0470 **(15.71%)**	0.0448 **(11.53%)**	0.0489 **(18.95%)**	0.0526 **(24.65%)**	0.0473 **(16.35%)**
h13	0.0311	0.0368 **(15.51%)**	0.0378 **(17.77%)**	0.0396 **(21.5%)**	0.0394 **(21.13%)**	0.388 **(19.91%)**

TABLE 4. TDD, 11th and 13th current harmonics forecast error for wind DFIG-PV model.

Forecasting Models	TDD		h7		h11		h13		Reference / Publication
	RMSE	MAE	RMSE	MAE	RMSE	MAE	RMSE	MAE	
LSTM-ANFIS Model	5.0956	2.7589	8.9003	6.6133	8.8975	7.4692	**6.4145**	**5.2047**	Proposed Model
ANFIS-LSTM Model	**4.6585**	**2.6165**	**8.2918**	**5.9852**	**8.4149**	**6.7443**	6.5160	5.2834	Proposed Model
LSTM	6.5412	4.1523	9.5897	7.3695	9.2142	7.5290	7.6975	5.8972	[27]
ANFIS	7.2423	5.7811	9.9177	7.6614	9.5265	7.8082	8.3274	6.6013	[26]
CRNNL	8.8514	5.7865	10.0224	7.7198	10.1251	8.1193	7.9709	6.2420	[22], [23] & [24]
CRNNG	7.0190	5.3318	9.8278	7.4801	10.0475	8.2530	9.0973	6.7163	[22], [23] & [24]
CRNNGL	7.1629	5.5188	9.7003	7.3899	10.4892	8.6382	8.1300	6.2536	[22], [23] & [24]

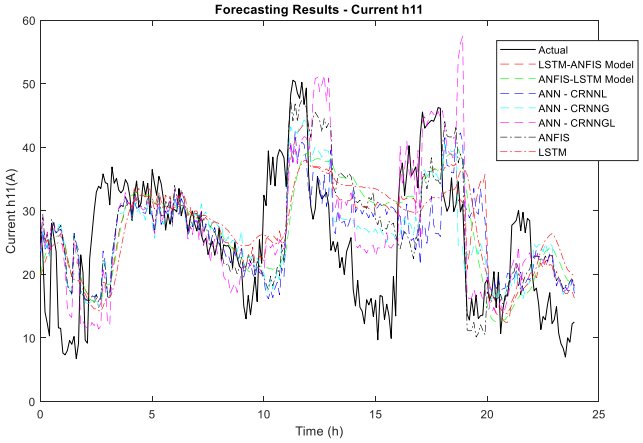

FIGURE 21. Current 11th harmonic – actual vs forecast curves wind DFIG_PV.

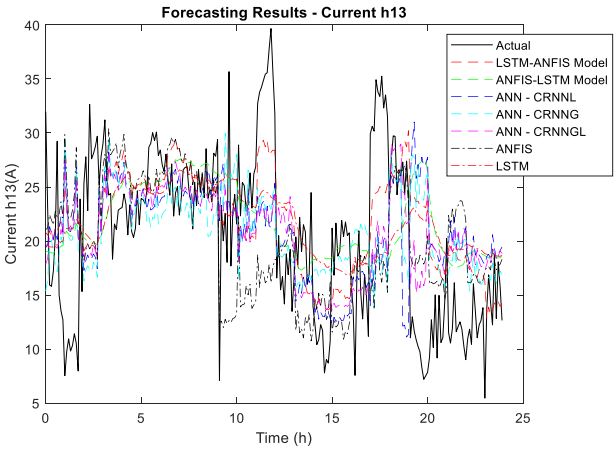

FIGURE 22. Current 13th harmonic – actual vs forecast curves wind DFIG_PV.

2) CURRENT HARMONICS

This section presents the actual versus forecasted curves for the individual forecasting methods in literature as well as the eight proposed hybrid models used to predict the TDD, h7, h11 and h13 harmonics. Figures 19, 20, 21 and 22 present the forecast curves followed by Tables 4 summarizing the performance of each model.

ANFIS-LSTM Model fits the actual curve better than the other models for TDD, h7 and h11 forecasts, as seen in Figures 19, 20 & 21. Table 4 shows that the lowest RMSE & MAE recorded for TDD (4.6585 & 2.6165), h7 (8.2918 & 5.9852) and h11 (8.4149 & 5.9852) respectively. The ANFIS-LSTM Model is also the second-best performing model for h13. The LSTM-ANFIS Model has the lowest RMSE & MAE for h13 (6.4145 & 5.2047). Furthermore, the LSTM has produced best results among the individual models for all current harmonic forecasting parameters. Moreover, like the results in voltage harmonics, both the hybrid models outperform the individual models in accuracy.

TABLE 5. Best forecasting model comparison for current harmonics – wind DFIG-PV.

Forecasting Parameter	ANFIS-LSTM Model RMSE	RMSE (% Improvement)				
		LSTM	ANFIS	CRNNL	CRNNG	CRNNGL
TDD	4.6585	6.5412 **(28.78%)**	7.2423 **(35.68%)**	8.8514 **(47.37%)**	7.019 **(33.63%)**	7.1629 **(34.96%)**
h7	8.2918	9.5897 **(13.53%)**	9.9177 **(16.39%)**	10.0224 **(17.27%)**	9.8278 **(15.63%)**	9.7003 **(14.52%)**
h11	8.4149	9.2142 **(8.67%)**	9.5265 **(11.67%)**	10.1251 **(16.89%)**	10.0475 **(16.25%)**	10.4892 **(19.78%)**
h13	6.5160	7.6975 **(15.35%)**	8.3274 **(21.75%)**	7.9709 **(18.25%)**	9.0973 **(28.37%)**	8.13 **(19.85%)**

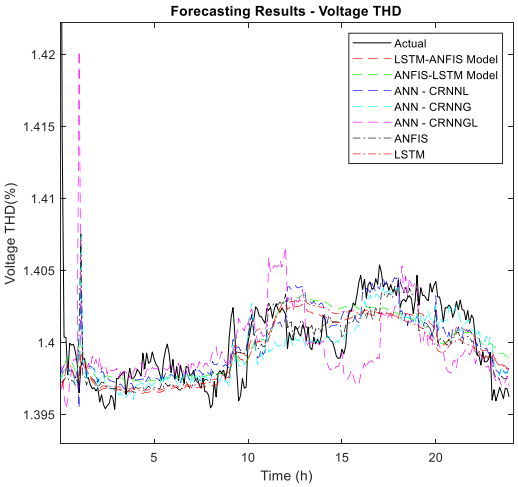

FIGURE 23. THDV – actual vs forecast curves wind PMSG-PV.

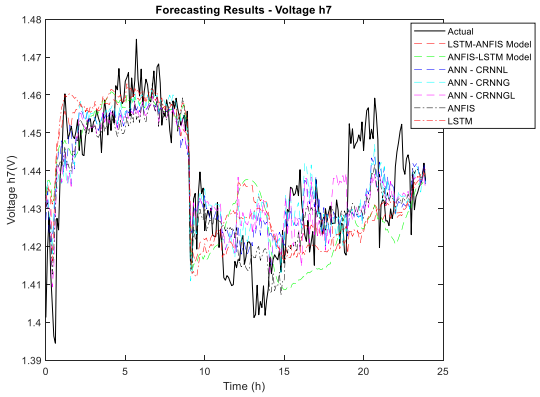

FIGURE 24. Voltage 7th harmonic – actual vs forecast curves wind PMSG_PV.

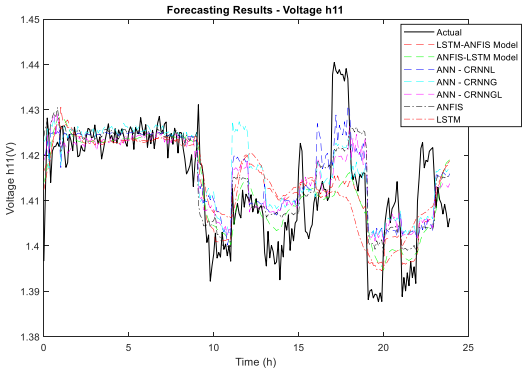

FIGURE 25. Voltage 11th harmonic – actual vs forecast curves wind PMSG_PV.

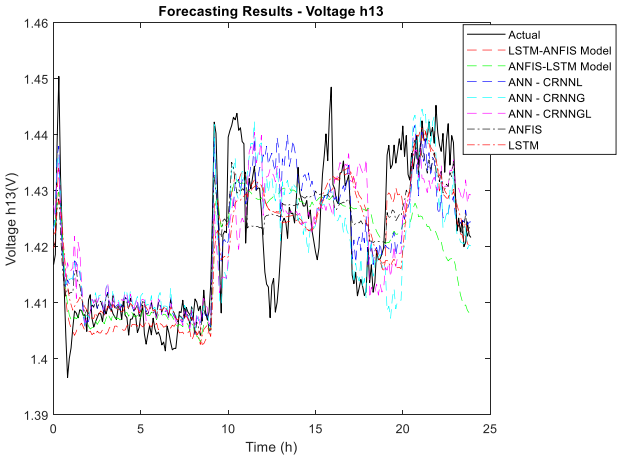

FIGURE 26. Voltage 13th harmonic – actual vs forecast curves wind PMSG_PV.

Furthermore, table 5 presents the percent improvement that ANFIS-LSTM model offers over the individual models tested. It is evident that the ANFIS-LSTM Model produces superior results over all other models. LSTM produces the best forecast as compared to all individual models. Hence, ANFIS-LSTM Model offers improvements over LSTM forecasts of 28.78%, 13.53%, 8.67% and 15.35% for THD, h7, h11 and h13 respectively. Likewise, the superior performance of model-8 over all other models is evident, it establishes that the proposed hybrid models are superior to the forecasting techniques used in the literature.

B. HARMONIC FORECASTING – WIND PMSG-PV MODEL

1) VOLTAGE HARMONICS

The actual versus predicted curves for all eight proposed hybrid models and the individual forecasting methods in literature for wind PMSG-PV generator are shown in Figures 23, 24, 25 & 26 for Voltage THD, 7th, 11^{th,} and 13th voltage

TABLE 6. THD, 11th and 13th voltage harmonics forecast error for wind PMSG-PV model.

Forecasting Models	THD		h7		h11		h13		Reference / Publication
	RMSE	MAE	RMSE	MAE	RMSE	MAE	RMSE	MAE	
LSTM-ANFIS Model	0.00422	0.00162	0.01018	0.00808	0.00798	0.00608	**0.007**	**0.00521**	Proposed Model
ANFIS-LSTM Model	**0.00421**	**0.00156**	**0.0097**	**0.0075**	**0.00767**	**0.00568**	0.00704	0.00556	Proposed Model
LSTM	0.00436	0.00192	0.01314	0.01005	0.00956	0.00734	0.00910	0.00674	[27]
ANFIS	0.00486	0.00247	0.01304	0.00962	0.00843	0.00630	0.00965	0.00742	[26]
CRNNL	0.00473	0.00220	0.01462	0.01141	0.00914	0.00690	0.00874	0.00651	[22], [23] & [24]
CRNNG	0.00447	0.00198	0.01140	0.00894	0.00894	0.00701	0.00918	0.00673	[22], [23] & [24]
CRNNGL	0.00483	0.00238	0.01209	0.00916	0.00861	0.00667	0.00983	0.00744	[22], [23] & [24]

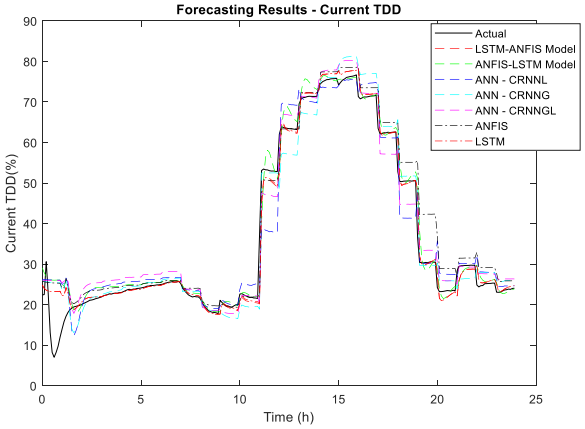

FIGURE 27. TDD – actual vs forecast curves wind PMSG-PV.

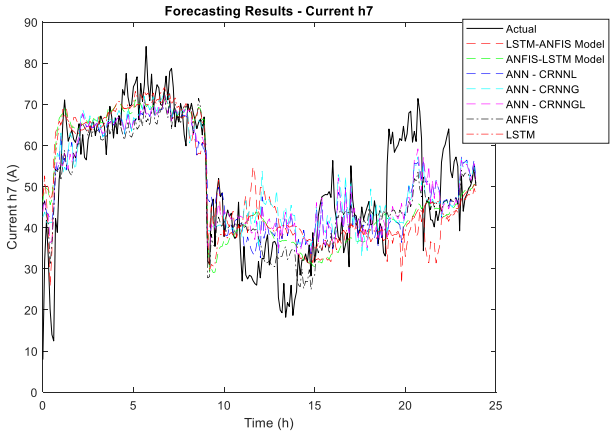

FIGURE 28. Current 7th harmonic – actual vs forecast curves wind PMSG_PV.

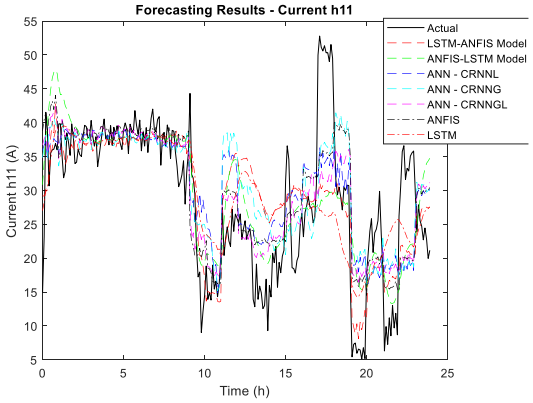

FIGURE 29. Current 11th harmonic – actual vs forecast curves wind PMSG_PV.

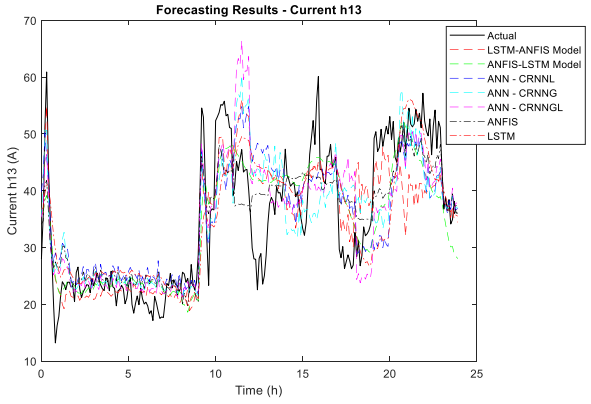

FIGURE 30. Current 13th harmonic – actual vs forecast curves wind PMSG_PV.

harmonics (h7, h11 & h13). The forecast results are followed by Table 6 summarizing the error profile of each forecast made for each variable.

By observing Table 6, it can be concurred that the overall performance of both proposed hybrid models has surpassed the forecast produced by any other individual models adopted in literature. It is obvious that the best performing model is ANFIS-LSTM model with the lowest RMSE of 0.00421 for THD, 0.0097 for h7 and 0.00767 for h11 respectively. Furthermore, the LSTM-ANFIS model produces the best results for h13 with RMSE of 0.007 and MAE of 0.00521. As for the individual models, for THD, the best performing model is LSTM, for h7 is CRNNG, for h11 ANFIS and for h13 CRNNL.

TABLE 7. Best forecasting model comparison for voltage harmonics – wind DFIG-PV.

Forecasting Parameter	ANFIS-LSTM Model RMSE	RMSE (% Improvement)				
		LSTM	ANFIS	CRNNL	CRNNG	CRNNGL
THD	0.00421	0.00436 **(3.39%)**	0.00486 **(13.41%)**	0.00473 **(10.99%)**	0.00447 **(5.93%)**	0.00483 **(12.95%)**
h7	0.0097	0.001314 **(26.18%)**	0.01304 **(25.59%)**	0.01462 **(33.64%)**	0.0114 **(14.9%)**	0.01209 **(19.75%)**
h11	0.00767	0.00956 **(19.76%)**	0.00843 **(8.97%)**	0.00914 **(16.06%)**	0.00894 **(14.13%)**	0.00861 **(10.87%)**
h13	0.00704	0.0091 **(22.58%)**	0.00965 **(27.02%)**	0.00874 **(19.4%)**	0.00918 **(23.27%)**	0.00983 **(28.3%)**

TABLE 8. THD, 11th and 13th current harmonics forecast error for wind DFIG-PV model.

Forecasting Models	THD		h7		h11		h13		Reference / Publication
	RMSE (%)	MAE (%)	RMSE (%)	MAE (%)	RMSE (%)	MAE (%)	RMSE (%)	MAE (%)	
LSTM-ANFIS Model	3.2268	1.5521	10.2656	7.8567	7.6828	5.5971	7.0060	5.3960	Proposed Model
ANFIS-LSTM Model	**3.2011**	**1.5157**	**9.5301**	**7.4151**	**7.2851**	**5.5141**	**6.3340**	**4.9965**	Proposed Model
LSTM	3.9070	2.1487	11.3811	8.2053	8.5276	6.2978	7.9486	5.8163	[27]
ANFIS	4.7846	3.0990	11.1411	8.2681	8.2793	6.4015	7.9227	5.8418	[26]
CRNNL	5.2654	3.4145	12.2311	8.9429	9.3007	7.2585	8.1233	6.1220	[22], [23] & [24]
CRNNG	6.1329	4.3554	12.0196	9.1486	8.3457	6.5548	8.1785	6.3640	[22], [23] & [24]
CRNNGL	4.8780	3.6053	11.5214	8.6189	7.8883	6.0364	7.9894	6.3652	[22], [23] & [24]

TABLE 9. Best forecasting model comparison for voltage harmonics – wind DFIG-PV.

Forecasting Parameter	ANFIS-LSTM Model RMSE	RMSE (% Improvement)				
		LSTM	ANFIS	CRNNL	CRNNG	CRNNGL
THD	3.2011	3.907 **(18.07%)**	4.7846 **(33.1%)**	5.2654 **(39.21%)**	6.1329 **(47.8%)**	4.878 **(34.38%)**
h7	9.5301	11.3811 **(16.26%)**	11.1411 **(14.46%)**	12.2311 **(22.08%)**	12.0196 **(20.71%)**	11.5214 **(17.28%)**
h11	7.2851	8.5276 **(14.57%)**	8.2793 **(12.01%)**	9.3007 **(21.67%)**	8.3457 **(12.71%)**	7.8883 **(7.65%)**
h13	6.334	7.9486 **(20.31%)**	7.9227 **(20.05%)**	8.1233 **(22.03%)**	8.1785 **(22.55%)**	7.9894 **(20.72%)**

Table 7 shows the error outline and percent improvement comparing the prediction of ANFIS-LSTM model and individual models tested. For THD, ANFIS-LSTM model offers 3.39% improvement over LSTM which is the best performing individual model. Similarly, for h7, the percent improvement is 14.9% in contrast with CRNNG forecast, for h11, 8.97% improvement over ANFIS and finally, for h13 there is 19.4% improvement as compared to CRNNL.

2) CURRENT HARMONICS

The actual vs anticipated curves for eight proposed hybrid models and five individual models adopted from literature used to predict the TDD, h7, h11, and h13 for wind PMSG-PV model current harmonics are presented in this section. The curves are contained in Figures 27, 28, 29 & 30 whereas the performance stats for forecast are presented in Table 8.

As observed in Table 8, the ANFIS-LSTM model produces the best results with lowest RMSE for TDD (3.2011), h7 (1.5157), h11 (7.2851) and h13 (6.334). Among individual models, LSTM produces the best results for TDD with RMSE 3.907, ANFIS for h7 (11.1411) and h13 (7.9227) and CRNNGL for h11 (7.8883). Moreover, to further analyze results table 9 presents the percent improvement of ANFIS-LSTM model results over all individual models.

With reference to the results presented in table 9, the percent improvement of ANFIS-LSTM model over individual models is evident. Comparing the performance with best performing individual model, for TDD ANFIS-LSTM model performance provides 18.07% improvement over LSTM, for h7 and h13 the percent improvement is 14.46% and 20.05% over ANFIS and for h11, ANFIS-LSTM model produces 7.65% improved results over CRNNGL.

VIII. CONCLUSION

In this study, two hybrid forecasting models were introduced for generating harmonic forecasts based on simulated data from Wind DFIG-PV and Wind PMSG-PV systems. The models predicted four voltage parameters (h7, h11, h13, and THD) and four current parameters (h7, h11, h13, and TDD) for each generator, resulting in sixteen distinct forecasting cases. To assess forecast accuracy, a comparative analysis was conducted by contrasting the proposed hybrid models with established forecasting techniques.

The hybrid models, designed in a meticulous two-stage configuration, incorporated a combination of LSTM and ANFIS techniques in stage-1 and stage-2. Specifically, the first model, LSTM-ANFIS, integrated LSTM in stage-1 and ANFIS in stage-2, while the second model, ANFIS-LSTM, followed a reverse structural arrangement. The evaluation included five individual models used by prior researchers, encompassing ANN variants (CRNNL, CRNNG & CRNNGL), ANFIS, and LSTM. Empirical findings revealed the consistent outperformance of the ANFIS-LSTM model over both the LSTM-ANFIS hybrid model and all individual models, emphasizing its superiority across the sixteen forecasting cases, such as Wind-DFIG PV and Wind-PMSG PV. This comparison effectively highlighted the distinct advantages of employing hybrid models and the percentage improvement they offer over traditional techniques.

The study provides an in-depth analysis of the advantages and disadvantages associated with the proposed hybrid forecasting models, particularly focusing on the ANFIS-LSTM configuration. Through a comprehensive evaluation of sixteen forecasting cases, the study clearly demonstrates the superiority of the ANFIS-LSTM hybrid model over individual models and alternative hybrid model, LSTM-ANFIS. This finding highlights the innovative nature of the proposed hybrid model in enhancing forecasting accuracy, which is crucial for the advancement of literature in this field.

One of the key advantages highlighted in the study is the consistent outperformance of the ANFIS-LSTM hybrid model across various forecasting scenarios. Specifically, in cases involving Wind-DFIG and Wind-PMSG systems, the ANFIS-LSTM model exhibited superior performance in predicting parameters such as voltage THD and current TDD at multiple time horizons. This consistent improvement underscores the effectiveness of hybrid approaches in forecasting and emphasizes the innovation brought about by integrating ANFIS and LSTM techniques.

Moreover, the study emphasizes the versatility of hybrid models by showcasing the integration of LSTM and ANFIS techniques in different configurations. This adaptability allows for a more nuanced approach to forecasting, utilizing the strengths of each technique in a complementary manner. Additionally, the comparison with individual models effectively highlights the clear advantages of employing hybrid models, showcasing the percentage improvement they offer over traditional techniques.

However, the study also acknowledges several limitations that warrant attention for a more comprehensive evaluation. It recognizes the need to ensure the consistency of model performance across diverse contexts and datasets beyond the specific conditions of the Halifax-NS, Canada dataset. Addressing potential limitations related to the generalizability of the proposed hybrid models is crucial for enhancing their practical applicability. Furthermore, the study identifies the lack of consideration for the impact of the grid in the forecasting models as a major limitation. This suggests the importance of incorporating grid modeling in MATLAB or utilizing historical power system data to mitigate this limitation and enhance the relevance of the models in real-world applications.

In conclusion, the study makes a distinctive contribution to the literature on harmonic forecasting by successfully integrating ANFIS and LSTM techniques within a hybrid model, resulting in enhanced forecasting accuracy. The innovation exhibited by the ANFIS-LSTM hybridization, along with the clear advantages demonstrated over individual models and an alternative hybrid model, enriches the literature and underscores the potential benefits of employing hybrid forecasting methodologies. However, the study's acknowledgment of the need for further research to address limitations and explore additional hybrid model combinations across varied scenarios reflects a commitment to advancing the domain of harmonic forecasting by utilizing the hybrid forecasting models in a responsible and rigorous manner.

REFERENCES

[1] P. F. Keebler, "Meshing power quality and electromagnetic compatibility for tomorrow's smart grid," *IEEE Electromagn. Compat. Mag.*, vol. 1, no. 2, pp. 100–103, 2nd Quart., 2012.

[2] P. M. Ivry, M. J. Rawa, D. W. P. Thomas, and M. Sumner, "Power quality of a voltage source converter in a smart grid," in *Proc. IEEE Grenoble Conf.*, Jun. 2013, pp. 1–6.

[3] F. Alhaddad, H. H. Aly, and M. El-Hawary, "An overview of active power filters for harmonics mitigation of renewable energies resources," in *Proc. IEEE 10th Annu. Inf. Technol., Electron. Mobile Commun. Conf. (IEMCON)*, Vancouver, BC, Canada, Oct. 2019, pp. 0386–0393.

[4] F. Al Hadi, H. H. H. Aly, and T. Little, "Harmonics prediction and mitigation using adaptive neuro fuzzy inference system model based on hybrid of wind solar driven by DFIG," in *Proc. IEEE 13th Annu. Inf. Technol., Electron. Mobile Commun. Conf. (IEMCON)*, Vancouver, BC, Canada, Oct. 2022.

[5] *IEEE Recommended Practice and Requirements for Harmonic Control in Electric Power Systems*, IEEE Standard 519-2014, 2014, pp. 1–29.

[6] *Limits for Harmonics Current Emissions (equipment Input Current < 16 A Per Phase)*, IEC Standard 61000-3-2, Int. Electrotech. Commission, 2005.

[7] T. Ortmeyer and K. Chakravarthi, "The effects of power system harmonics on power system equipment and loads," *IEEE Trans. Power Appl. Syst.*, vol. PAS-104, no. 9, pp. 2555–2563, Sep. 1985.

[8] J.-S.-R. Jang, "ANFIS: Adaptive-network-based fuzzy inference system," *IEEE Trans. Syst., Man, Cybern.*, vol. 23, no. 3, pp. 665–685, Aug. 1993, doi: 10.1109/21.256541.

[9] S. Hochreiter and J. Schmidhuber, "Long short-term memory," *Neural Comput.*, vol. 9, no. 8, pp. 1735–1780, Nov. 1997, doi: 10.1162/neco.1997.9.8.1735.

[10] A. B. Nassif, W. Xu, and W. Freitas, "An investigation on the selection of filter topologies for passive filter applications," *IEEE Trans. Power Del.*, vol. 24, no. 3, pp. 1710–1718, Jul. 2009.

[11] D. Bohaichuk, C. Muskens, and W. Xu, "Mitigation of harmonics in oil field electric systems using a centralized medium voltage filter," in *Proc. 9th Int. Conf. Harmon. Quality Power*, 2000, pp. 614–618.

[12] C.-J. Chou, C.-W. Liu, J.-Y. Lee, and K.-D. Lee, "Optimal planning of large passive-harmonic-filters set at high voltage level," *IEEE Trans. Power Syst.*, vol. 15, no. 1, pp. 433–441, Feb. 2000.

[13] A. Yazdani and R. Iravani, *Voltage-Sourced Converters in Power Systems: Modeling, Control, and Applications*. Hoboken, NJ, USA: Wiley, 2010.

[14] H. H. H. Aly, "Intelligent optimized deep learning hybrid models of neuro wavelet, Fourier series and recurrent Kalman filter for tidal currents constitutions forecasting," *Ocean Eng.*, vol. 218, Dec. 2020, Art. no. 108254, doi: 10.1016/j.oceaneng.2020.108254.

[15] P. K. Ray, P. S. Puhan, and G. Panda, "Real time harmonics estimation of distorted power system signal," *Int. J. Electr. Power Energy Syst.*, vol. 75, pp. 91–98, Feb. 2016.

[16] M. Kamenetsky and B. Widrow, "A variable leaky LMS adaptive algorithm," in *Proc. Conf. Rec. 38th Asilomar Conf. Signals, Syst. Comput.*, Pacific Grove, CA, USA, 2004, pp. 125–128, doi: 10.1109/acssc.2004.1399103.

[17] P. M. Ivry, O. A. Oke, D. W. P. Thomas, and M. Sumner, "Predicting harmonic distortion of multiple converters in a power system," *J. Electr. Comput. Eng.*, vol. 2017, pp. 1–10, Jan. 2017.

[18] M. M. H. Alhaj, N. M. Nor, V. S. Asirvadam, and M. F. Abdullah, "Comparison of power system harmonic prediction," *Proc. Technol.*, vol. 11, pp. 628–634, Jan. 2013.

[19] P. Rodríguez-Pajarón, A. Hernández Bayo, and J. V. Milanović, "Forecasting voltage harmonic distortion in residential distribution networks using smart meter data," *Int. J. Electr. Power Energy Syst.*, vol. 136, Mar. 2022, Art. no. 107653.

[20] W. S. McCulloch and W. Pitts, "A logical calculus of ideas immanent in nervous activity," *Bull. Math. Biophys.*, vol. 5, no. 4, pp. 115–133, Dec. 1943.

[21] H. Mori and S. Suga, "Power system harmonics prediction with an artificial neural network," in *Proc. IEEE Int. Symp. Circuits Syst. (ISCAS)*, Sep. 1991, pp. 1129–1132.

[22] J. J. Hopfield, "Neural networks and physical systems with emergent collective computational abilities," *Proc. Nat. Acad. Sci. USA*, vol. 79, no. 8, pp. 2554–2558, Apr. 1982, doi: 10.1073/pnas.79.8.2554.

[23] M. Žnidarec, Z. Klaić, D. Šljivac, and B. Dumnić, "Harmonic distortion prediction model of a grid-tie photovoltaic inverter using an artificial neural network," *Energies*, vol. 12, no. 5, p. 790, Feb. 2019.

[24] F. Rosenblatt, "The perceptron: A probabilistic model for information storage and organization in the brain," *Psychol. Rev.*, vol. 65, no. 6, pp. 386–408, 1958, doi: 10.1037/h0042519.

[25] M. Panoiu, C. Panoiu, and L. Ghiormez, "Neuro-fuzzy modeling and prediction of current total harmonic distortion for high power nonlinear loads," in *Proc. Innov. Intell. Syst. Appl. (INISTA)*, Jul. 2018, pp. 1–7.

[26] L. Shengqing, Z. Huanyue, X. Wenxiang, and L. Weizhou, "A harmonic current forecasting method for microgrid HAPF based on the EMD-SVR theory," in *Proc. 3rd Int. Conf. Intell. Syst. Design Eng. Appl.*, Jan. 2013, pp. 70–72.

[27] C. Cortes and V. Vapnik, "Support-vector networks," *Mach. Learn.*, vol. 20, pp. 273–297, Sep. 1995.

[28] E. M. Kuyunani, A. N. Hasan, and T. Shongwe, "Improving voltage harmonics forecasting at a wind farm using deep learning techniques," in *Proc. IEEE 30th Int. Symp. Ind. Electron. (ISIE)*, Jun. 2021, pp. 1–6.

[29] A. Y. Hatata and M. Eladawy, "Prediction of the true harmonic current contribution of nonlinear loads using NARX neural network," *Alexandria Eng. J.*, vol. 57, no. 3, pp. 1509–1518, Sep. 2018.

[30] S. Chen and S. A. Billings, "Representations of non-linear systems: The NARMAX model," *Int. J. Control*, vol. 49, no. 3, pp. 1013–1032, Mar. 1989, doi: 10.1080/00207178908559683.

[31] Y. Pang, "Short-term harmonic forecasting and evaluation affected by electrified railways on the power grid based on stack auto encoder neural network method and the comparison to BP method," in *Proc. 13th IEEE Conf. Ind. Electron. Appl. (ICIEA)*, May 2018, pp. 1159–1165.

[32] A. J. Zavala and A. R. Messina, "Dynamic harmonic regression approach to wind power generation forecasting," in *Proc. IEEE PES Transmiss. Distrib. Conf. Expo.*, Sep. 2016, pp. 1–6.

[33] *Wind Farm—DFIG Detailed Model*, MATLAB & Simulink, 2022.

[34] *MODEL Detailed Modelling of a 1.5 mw Wind Turbine Based on Direct-Driven PMSG*, 2020.

[35] *DATASET Typical Meteorological Data Access Service*, 2022.

[36] J. W. Cooley and J. W. Tukey, "An algorithm for the machine calculation of complex Fourier series," *Math. Comput.*, vol. 19, no. 90, pp. 297–301, Jan. 1965, doi: 10.1090/s0025-5718-1965-0178586-1.

[37] T. Takagi and M. Sugeno, "Fuzzy identification of systems and its applications to modeling and control," *IEEE Trans. Syst., Man, Cybern.*, vols. SMC–15, no. 1, pp. 116–132, Jan. 1985, doi: 10.1109/TSMC.1985.6313399.

[38] F. AlHadi, "Harmonics forecasting for wind and solar renewable energy resources-based electrical power systems," Ph.D. thesis, Dalhousie Univ., 2023.

[39] S. A. Ludwig, "Comparison of time series approaches applied to greenhouse gas analysis: ANFIS, RNN, and LSTM," in *Proc. IEEE Int. Conf. Fuzzy Syst. (FUZZ-IEEE)*, Jun. 2019, pp. 1–6.

[40] R. R. Yager and D. P. Filev, "Generation of fuzzy rules by mountain clustering," *J. Intell. Fuzzy Syst.*, vol. 2, no. 3, pp. 209–219, 1994.

[41] S. M. M. Alam and Mohd. H. Ali, "A new subtractive clustering based ANFIS system for residential load forecasting," in *Proc. IEEE Power Energy Soc. Innov. Smart Grid Technol. Conf. (ISGT)*, Feb. 2020, pp. 1–5.

[42] R. Kohavi, "A study of cross-validation and bootstrap for accuracy estimation and model selection," in *Proc. Int. Joint Conf. Artif. Intell.*, vol. 14, 2021.

[43] C. Willmott and K. Matsuura, "Advantages of the mean absolute error (MAE) over the root mean square error (RMSE) in assessing average model performance," *Climate Res.*, vol. 30, pp. 79–82, Jan. 2005, doi: 10.3354/cr030079.

[44] T. Chai and R. R. Draxler, "Root mean square error (RMSE) or mean absolute error (MAE)," *Geosci. Model Develop.*, vol. 7, no. 3, pp. 1247–1250, 2014, doi: 10.5194/gmdd-7-1525-2014.

[45] A. de Myttenaere, B. Golden, B. Le Grand, and F. Rossi, "Mean absolute percentage error for regression models," *Neurocomputing*, vol. 192, pp. 38–48, Jun. 2016, doi: 10.1016/j.neucom.2015.12.114.

FAWAZ M. AL HADI received the B.Sc. degree in electrical engineering from Riyadh College of Technology, Saudi Arabia, in 2007, and the M.A.Sc. and Ph.D. degrees from Dalhousie University, Canada, in 2014 and 2023 respectively. He is currently a Lecturer with Najran College of Technology, Saudi Arabia. His research interest includes renewable energy integration.

HAMED H. ALY (Senior Member, IEEE) received the B.Eng. and M.A.Sc. degrees (Hons.) in electrical engineering from Zagazig University, Egypt, in 1999 and 2005, respectively, and the Ph.D. degree from Dalhousie University, Canada, in 2012. He was a Postdoctoral Research Associate for one year and an Instructor for three years with Dalhousie University. He was with Acadia University, as an Assistant Professor, for three years. He is currently an Assistant Professor with Dalhousie University. His research interests include micro grids, smart grids, distributed generation, power quality issues, applications of artificial intelligence in power systems, energy management, green energy, and optimization.